Available online at www.sciencedirect.com
ScienceDirect
Developmental Biology 307 (2007) 300–313
DEVELOPMENTAL BIOLOGY
www.elsevier.com/locate/ydbio

FGF9 regulates early hypertrophic chondrocyte differentiation and skeletal vascularization in the developing stylopod

Irene H. Hung [1], Kai Yu, Kory J. Lavine, David M. Ornitz *

Department of Molecular Biology and Pharmacology, Washington University School of Medicine, Campus Box 8103, 660 S. Euclid Avenue, St. Louis, MO 63110, USA

Received for publication 1 March 2007; revised 5 April 2007; accepted 30 April 2007
Available online 6 May 2007

Abstract

Gain-of-function mutations in fibroblast growth factor (FGF) receptors result in chondrodysplasia and craniosynostosis syndromes, highlighting the critical role for FGF signaling in skeletal development. Although the FGFRs involved in skeletal development have been well characterized, only a single FGF ligand, FGF18, has been identified that regulates skeletal development during embryogenesis. Here we identify *Fgf9* as a second FGF ligand that is critical for skeletal development. We show that *Fgf9* is expressed in the proximity of developing skeletal elements and that *Fgf9*-deficient mice exhibit rhizomelia (a disproportionate shortening of proximal skeletal elements), which is a prominent feature of patients with FGFR3-induced chondrodysplasia syndromes. Although *Fgf9* is expressed in the apical ectodermal ridge in the limb bud, we demonstrate that the $Fgf9^{-/-}$ limb phenotype results from loss of FGF9 functions after formation of the mesenchymal condensation. In developing stylopod elements, FGF9 promotes chondrocyte hypertrophy at early stages and regulates vascularization of the growth plate and osteogenesis at later stages of skeletal development.

Keywords: Fibroblast growth factor 9 (FGF9); Skeletal development; Growth plate; Chondrocyte; Osteoblast; Periosteum; Perichondrium; Vascular development

Introduction

Fibroblast growth factor (FGF) signaling is essential for vertebrate limb development, from the initial formation and outgrowth of the limb bud to patterning and growth of the skeletal elements (Mariani and Martin, 2003; Min et al., 1998; Niswander, 2003;Ohuchi et al., 1997). The early phases of limb induction require the expression of *Fgf10* in lateral plate mesoderm, which activates *FGFR2b* in the overlying epithelium. Subsequently, *Fgf8* is expressed in the apical ectodermal ridge (AER) along with *Fgfs 4*, *9* and *17* (Colvin et al., 1999; Martin, 1998; Maruoka et al., 1998). Signals emanating from this specialized ectoderm are required for proximal-to-distal limb outgrowth, as well as maintenance of mesenchymal gene expression in the limb bud. Previous studies have shown that conditional inactivation of *Fgf8* ($Fgf8^{cko}$) in the AER at early stages results in hypoplasia or agenesis of proximal limb elements as well as less severe abnormalities in the intermediate and distal elements (Lewandoski et al., 2000; Moon and Capecchi, 2000). Conditional inactivation of both *Fgfs 4* and *8* ($Fgf4/8^{cko}$) in the AER ultimately results in limb agenesis; however, small limb buds do form initially. The defects in the proximal skeletal elements of the $Fgf8^{cko}$ and $Fgf4/8^{cko}$ animals are thought to result from the dramatic increase in apoptosis observed in the proximal limb bud mesenchyme (Boulet et al., 2004; Sun et al., 2002).

After limb bud initiation and outgrowth, development of the appendicular skeleton occurs via endochondral ossification, with cartilage anlagen prefiguring the future bone (Erlebacher et al., 1995; Karsenty and Wagner, 2002). Following formation of mesenchymal condensations, cells within these condensations differentiate into proliferating chondrocytes which elaborate an extracellular matrix rich in type II collagen, while

* Corresponding author.
E-mail address: dornitz@wustl.edu (D.M. Ornitz).
[1] Current address: University of Utah School of Medicine, Department of Neurobiology and Anatomy, Children's Health Research Center, and Department of Pediatrics, Room 401 MREB, 20 North 1900 East, Salt Lake City, Utah 84132-3401, USA.

0012-1606/$ - see front matter © 2007 Elsevier Inc. All rights reserved.
doi:10.1016/j.ydbio.2007.04.048

cells at the periphery differentiate into the surrounding perichondrium. As the cartilaginous template elongates, chondrocytes within the anlagen mature and hypertrophy, secreting a matrix rich in type X collagen. Concomitantly, skeletal vascularization is stimulated by angiogenic growth factors such as vascular endothelial growth factors (VEGF) (Gerber et al., 1999; Zelzer and Olsen, 2005) produced in the perichondrium and hypertrophic cartilage. These changes allow perichondrial angiogenesis to occur and, subsequently, invasion of blood vessels, osteoblasts, and osteoclasts into the avascular cartilaginous template to form the primary ossification center. In a separate, but related, process, osteoprogenitor cells in the perichondrium differentiate into osteoblasts to form cortical bone. These events: chondrogenesis, vascularization and osteogenesis, are coordinated by multiple signaling molecules including IHH, PTHrP, VEGF and FGF to regulate skeletogenesis (de Crombrugghe et al., 2001; Karsenty and Wagner, 2002; Ornitz and Marie, 2002; Zelzer and Olsen, 2005).

Multiple human skeletal dysplasia syndromes result from activating mutations in FGF receptors, highlighting the critical role for FGF signaling in bone development. For example, chondrodysplasias such as achondroplasia, hypochondroplasia and thanatophoric dysplasia are due to mutations in FGFR3 (Bellus et al., 1995; Rousseau et al., 1994; Shiang et al., 1994; Tavormina et al., 1995). The limb dysmorphology of these patients is characterized by rhizomelic shortening, with proximal elements affected more severely than intermediate and distal elements. Various craniosynostosis syndromes are caused by activating mutations in FGFR1–3 and result in premature fusion of the cranial sutures (Britto et al., 2001; Cohen, 2000; Morriss-Kay and Wilkie, 2005; Wilkie, 1997, 2000). Afflicted patients also exhibit variable abnormalities in limb development in addition to their calvarial deformities. Despite the identification and functional characterization of the FGFRs involved in skeletogenesis, to date only two of the 22 known FGFs, FGF2 and FGF18, have been shown to have functional roles in skeletal development.

Fgf18 is expressed in the perichondrium and joint spaces and regulates early stages of cartilage development by promoting chondrocyte proliferation and differentiation while, at later stages, FGF18 functions to inhibit chondrogenesis by signaling to FGFR3. Additionally, FGF18 promotes skeletal vascularization by inducing *Vegf* expression and positively regulates osteogenesis by signaling to FGFR 1 and 2 in the developing perichondrium/periosteum (Liu et al., 2002, 2007; Ohbayashi et al., 2002). Besides *Fgf18*, expression of *Fgfs 7*, *8* and *17* has also been observed in the perichondrium; however, gene targeting experiments have not elucidated roles for these ligands in skeletal development (Finch et al., 1995; Mason et al., 1994; Xu et al., 1999). *Fgf2* expression has been demonstrated in proliferating and prehypertrophic chondrocytes, periosteal cells and osteoblasts (Hurley et al., 1994, 1999; Sabbieti et al., 1999, 2005; Sullivan and Klagsbrun, 1985). Mice lacking *Fgf2* have defects in osteogenesis, which result in aberrant trabecular bone formation (Montero et al., 2000). The identification of additional endogenous FGF ligand(s) for FGFRs expressed in bone has been problematic, likely due to functional redundancy between ligands or, alternatively, activity restricted to specific skeletal elements or to limited developmental stages.

Fgf9 is expressed in the AER of the developing limb bud and in migrating myoblasts (Colvin et al., 1999). *Fgf9* transcripts have also been observed surrounding and within precursor skeletal elements at E12.5 and E14.5 (Garofalo et al., 1999). Here we show *Fgf9* expression localized to the perichondrium/periosteum, trabecular bone, muscle and loose mesenchyme surrounding developing bone. Mice lacking *Fgf9* ($Fgf9^{-/-}$) exhibit rhizomelia, a prominent limb patterning defect observed in patients afflicted with achondroplasia. In *Fgf9*-deficient mice, the hindlimb femora are affected more severely than the forelimb humeri. The $Fgf9^{-/-}$ limb phenotype can be interpreted as a consequence of loss of *Fgf9* expression in the AER resulting in a skeletal patterning defect that primarily affects mesenchymal condensations, or loss of *Fgf9* expression at later stages of skeletogenesis directly affecting chondrogenesis, osteogenesis and/or vascularization of proximal skeletal elements. Here we demonstrate that $Fgf9^{-/-}$ mice have normal limb bud development and mesenchymal condensations, but in stylopod elements, decreased chondrocyte proliferation, delayed initiation of chondrocyte hypertrophy and abnormal osteogenesis secondary to defects in skeletal vascularization.

Materials and methods

Skeletal preparations and bone morphometric analysis

Skeletons were prepared as described previously (Colvin et al., 1996) using Alizarin red S and Alcian blue (Sigma) staining to visualize mineralized bone and cartilage, respectively. Lengths of individual bones were measured at E18.5 using Canvas X (ACD Systems) software.

Generation of mice

$Fgf9^{-/-}$ and $Fgfr3^{-/-}$ mice were generated as described (Colvin et al., 1996; Colvin et al., 2001). Conditional alleles for FGFR1 and FGFR2 have been previously described (Pirvola et al., 2002; Yu et al., 2003). Mice homozygous for conditional alleles of both FGFR1 and FGFR2 ($Fgfr1^{flox/flox}$;$Fgfr2^{flox/flox}$) were crossed with mice carrying one copy of *Dermo-1-cre* (Yu et al., 2003) and heterozygous for null alleles of FGFR1 and FGFR2 ($Fgfr1^{\Delta/+}$;$Fgfr2^{\Delta/+}$;*cre*/+) to obtain litters containing wild-type, $Fgfr1^{cko}$ and $Fgfr2^{cko}$ embryos. Note that *Fgfr1* and *Fgfr2* single *CKO* embryos are also missing one functional allele of *FGFR2* and *FGFR1*, respectively.

Histological analysis, immunohistochemistry and in situ hybridization

Tissues were fixed in 4% paraformaldehyde. Histomorphometry was carried out on hematoxylin and eosin (H&E)-stained 5 μm paraffin sections using AxioVision 3.0 software (Zeiss). Hypertrophic zone heights were measured along the midline of the distal femoral and proximal tibial growth plates at E17.5 and E18.5. At least 3 sections were measured for each embryo. Mineralized bone was visualized by von Kossa staining with methyl green counterstaining. For PECAM (CD31) immunohistochemistry, embryos were fixed in 4% paraformaldehyde followed by 20% sucrose infiltration. Tissues were embedded in OCT (Tissue-Tek®) and 10-μm cryostat sections were made. Sections were fixed in 0.2% glutaraldehyde prior to peroxidase blocking with 3% H_2O_2 in methanol. The primary antibody was anti-PECAM (BD PharMingen). Secondary antibody was biotinylated anti-rat IgG (BD PharMingen). Immunoreactivity detection was performed using a streptavidin–biotin–peroxidase complex (sABC-HRP, DakoCytomation K0377) and DAB (Zymed). Sections were counterstained with hematoxylin. Whole-mount *in situ* hybridization was

performed according to standard protocol. Radioactive *in situ* hybridization was performed as described (Naski et al., 1998).

Analysis of cell proliferation and apoptosis

Anti-bromodeoxyuridine (BrdU) immunohistochemistry was carried out as described (Naski et al., 1998). BrdU-positive nuclei of reserve and proliferating chondrocytes were counted and the area of the reserve and proliferating chondrocyte zones was measured using ImageJ 1.36b software (NIH). The number of BrdU-positive nuclei per 0.01 mm^2 area was calculated for each embryo examined. At least three sections were analyzed through a 10× objective for each embryo. TUNEL assay was performed using the In Situ Cell Death Detection Kit, POD (Roche) per manufacturer's instructions.

Embryonic limb explant cultures

Forelimb cartilage was dissected from E14.5 VEGF-*LacZ* mouse embryos (Miquerol et al., 1999) and placed at the air-fluid interface on Transwell filters (Corning) containing DMEM with 10% fetal calf serum (GibcoBRL), antibiotic antimycotic solution (Sigma) and 2 μg/ml heparin. Media were supplemented with 250 ng/ml recombinant FGF10 (PeproTech), recombinant FGF9 (PeproTech) or BSA. Explants were cultured for 2 days at 37 °C/5% CO_2 under humidified conditions.

Limb explant histochemistry and immunohistochemistry

Whole-mount β-galactosidase staining was performed as described (Liu et al., 2007). After post-fixing in 4% paraformaldehyde, the explants were infiltrated with 20% sucrose and embedded in OCT at −20 °C for sectioning. Frozen sections (8 μm) were mounted in toluene-based media. The contralateral limb explant was used for PECAM whole-mount immunohistochemistry as described (Lavine et al., 2006). For histological analysis, 5-μm paraffin sections of stained explants were counterstained with hematoxylin.

Results

Loss of Fgf9 affects the proximal skeletal elements of the developing limb

Comparison of Alizarin red- and Alcian blue-stained skeletons of E18.5 and P0 mice showed that the skeletons of $Fgf9^{-/-}$ mice were approximately 10–15% smaller than littermate controls. Although the general patterning of the $Fgf9^{-/-}$ skeletal elements resembled that of control animals, the $Fgf9^{-/-}$ hindlimb proximal elements were disproportionately shorter, while the intermediate and distal elements of the limbs appeared unaffected (Figs. 1A, B). $Fgf9^{-/-}$ mice also lacked the third trochanter (Fig. 1C), normally located on the lateral aspect of the femur (Bateman, 1954). Additionally, closer examination of the $Fgf9^{-/-}$ humerus revealed an enlarged deltoid tuberosity (Fig. 1A). Thus, bone growth and patterning defects were observed in the stylopod elements of $Fgf9^{-/-}$ mice. In comparison with controls, the Alizarin red-stained region of the $Fgf9^{-/-}$ femur appeared smaller, suggesting that bony mineralization was decreased.

Morphometric analyses were performed on limb skeletal preparations of $Fgf9^{-/-}$ and littermate controls at E18.5. In the forelimb, the mutant humerus length was not significantly shorter (92% of control, $n=3$, $p=0.06$). In the hindlimb, the mutant femur length was significantly decreased (82% of control, $n=3$, $p=0.008$). Because the entire skeleton of $Fgf9^{-/-}$ mice was 10–15% smaller than that of control animals, we compared ratios of limb element lengths to determine whether the proximal elements of the limbs were disproportionately reduced compared to the intermediate limb compartment. In the forelimb, the ratio of humerus to radius or ulna length did not reveal a significant difference between $Fgf9^{-/-}$ and control mice (data not shown). However, the femur to tibia ratio showed a significantly smaller hindlimb stylopod in $Fgf9^{-/-}$ mice compared to control (control femur/tibia (F/T) ratio = 0.96 ± 0.03; $Fgf9^{-/-}$ F/T ratio = 0.85 ± 0.04; $p=0.013$, $n=3$) (Fig. 1D).

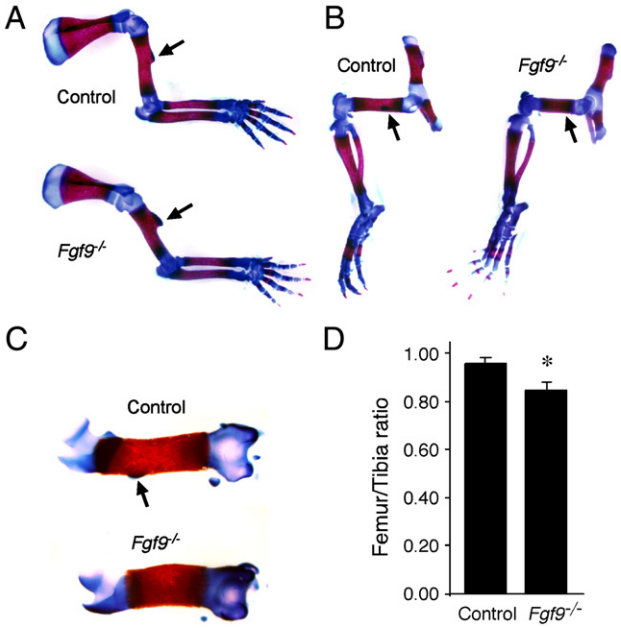

Fig. 1. Proximal limb development in $Fgf9^{-/-}$ mice. (A, B) Skeletal preparations of control and $Fgf9^{-/-}$ forelimbs (A) and hindlimbs (B) at P0. Note enlarged deltoid tuberosity (arrows) in the $Fgf9^{-/-}$ humerus. The $Fgf9^{-/-}$ femur is significantly shorter than control with a smaller region of Alizarin red staining. The third trochanter is missing on the lateral aspect of the femur (arrows in panel B). (C) Higher magnification of femora from (B) to show absence of third trochanter (arrow) in $Fgf9^{-/-}$ mice. (D) Comparison of femur to tibia length ratios between control and $Fgf9^{-/-}$ hindlimbs shows statistically significant reduction in length ratio for $Fgf9^{-/-}$ limb. *Student's T test, $n=3$, $p=0.013$.

Fgf9 expression during limb development

Previous studies have localized *Fgf9* expression to the AER of the developing limb bud at E10.5 and to skeletal myoblasts at E10.5–E12.5 (Colvin et al., 1999). *Fgf9* expression has also been observed at later stages during skeletal development in regions corresponding to mesenchymal condensations in the limb at E12.5 and in mesenchyme surrounding rib condensations at E14.5 (Garofalo et al., 1999). Our examination of spatial and temporal patterns of *Fgf9* expression in the limb showed that, at E12.5, *Fgf9* was expressed in the mesenchyme surrounding the cartilaginous condensations; however, its expression was excluded from the condensations (Figs. 2A, B). At later stages of limb development, *Fgf9* was expressed in the perichondrium/periosteum, as well as in surrounding skeletal muscle and overlying skin (Figs. 2C–F). Low levels of *Fgf9* mRNA were also detectable in the primary spongiosa at this

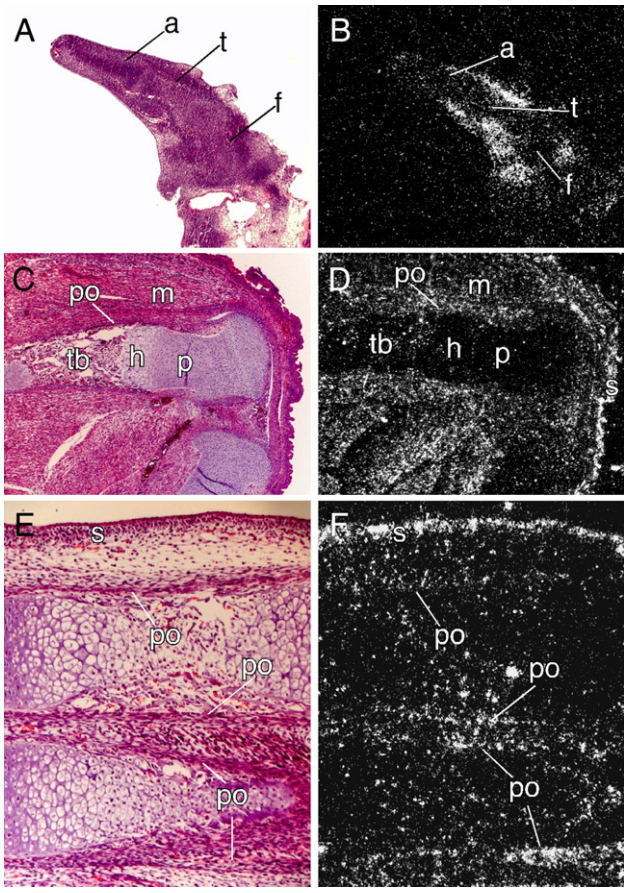

Fig. 2. *Fgf9* expression patterns in the developing limb. (A) Longitudinal section through the hindlimb of an E12.5 embryo stained with hematoxylin and eosin (H&E). (B) *Fgf9 in situ* hybridization of a nearby section to that shown in panel A. Note *Fgf9* transcripts are excluded from the condensations (f—femur, t—tibia, a—autopod). (C) H&E staining of longitudinal section through femur and proximal tibia at E16.5. (D) Nearby section to panel C showing *Fgf9* expression in the perichondrium/periosteum (po), trabecular bone (tb), surrounding muscle (m) and skin (s) but not in proliferating (p) or hypertrophic (h) chondrocytes. (E) H&E staining of a longitudinal section through the ulna (top) and radius (bottom) at E15.5. (F) Nearby section to panel E showing *Fgf9* expression in the perichondrium/periosteum (po) and skin (s).

stage. This expression pattern suggests that *Fgf9* could regulate multiple stages of skeletogenesis since, like *Fgf18* (Liu et al., 2002; Ohbayashi et al., 2002), this ligand is juxtaposed to *Fgfr3*-expressing proliferating chondrocytes, *Fgfr1*-expressing hypertrophic chondrocytes and *Fgfr1* and *Fgfr2*-expressing cells in the perichondrium and periosteum (Naski and Ornitz, 1998; Orr-Urtreger et al., 1991; Peters et al., 1992, 1993). Additionally, *Fgf9* expression in the skeletal musculature surrounding bone could serve as an additional source of ligand that may also impact skeletal development.

Loss of Fgf9 from the AER does not cause limb patterning defects

Transgenic mice with reduced AER-FGF signaling due to a conditional loss of *Fgf8* ($Fgf8^{cko}$) or a combination of *Fgfs 4* and *8* ($Fgf4/8^{cko}$) from the AER have shortened or absent proximal limb elements (Boulet et al., 2004; Lewandoski et al., 2000; Moon and Capecchi, 2000; Sun et al., 2002). These mice also had smaller limb bud sizes and decreased expression of mesenchymal limb bud genes. Although the $Fgf9^{-/-}$ mice have stylopod element defects similar to those observed in the $Fgf8^{cko}$ and $Fgf4/8^{cko}$ mice, the $Fgf9^{-/-}$ limb buds appeared normal in size between E9.5 and E11.5 (Figs. 3A–F and data not shown). To determine whether any molecular changes were detectable in $Fgf9^{-/-}$ limb buds, the expression patterns of *Fgf8* and *Shh* were examined by whole-mount *in situ* hybridization. Similar levels of *Fgf8* expression were observed in $Fgf9^{-/-}$ and control limb buds (Figs. 3A, B). *Shh* (important for anterior–posterior (AP) patterning and AER maintenance) expression in the posterior limb mesenchyme requires AER-FGF signaling (Laufer et al., 1994; Niswander et al., 1994; Zuniga et al., 1999). *Shh* expression levels appeared slightly decreased and diffuse in $Fgf9^{-/-}$ limb buds compared to controls (Figs. 3C, D). In the $Fgf4/8^{cko}$ embryos, increased apoptosis in proximal limb mesenchyme was observed, which was hypothesized to result in a smaller proximal mesenchymal condensation and consequently smaller proximal skeletal elements. At E10.5 and E11.5, we observed similar levels of apoptosis in the proximal limb bud and in the AER of control and $Fgf9^{-/-}$ mice (Figs. 3E, F and data not shown). Together, these data suggest that AER-FGF function is preserved in $Fgf9^{-/-}$ mice and that FGFs 4, 8 and 17 can functionally compensate for any loss of FGF9 signaling.

Defects in AER-FGF signaling resulted in reduced proximal condensation sizes during early limb development in $Fgf8^{cko}$ and $Fgf4/8^{cko}$ mice. However, in $Fgf9^{-/-}$ mice, histological sections revealed that mesenchymal condensations corresponding to proximal, intermediate and distal skeletal elements appeared normal in size and shape at E12.5 (Figs. 3G, H). Although *Shh* expression was slightly decreased in the $Fgf9^{-/-}$ limb bud, $Fgf9^{-/-}$ autopod elements were indistinguishable from controls, suggesting that normal SHH signaling was present. Additionally, *Sox9*, a marker of prechondrogenic condensations, was expressed at control levels in $Fgf9^{-/-}$ limb condensations (Figs. 3I, J). Levels of type II collagen (*ColII*) expression in $Fgf9^{-/-}$ mice appeared similar to controls (Figs. 3K, L), indicating that mesenchymal cells within the condensations were undergoing chondrogenic differentiation. These data demonstrate that mesenchymal aggregation and condensation, as well as early stages of chondrogenic differentiation, are not significantly altered during the initial stages of limb development in $Fgf9^{-/-}$ mice and suggest that loss of *Fgf9* from the AER does not cause the observed rhizomelic phenotype.

Delayed skeletogenesis in $Fgf9^{-/-}$ proximal limb elements

Histological analyses at later stages of limb development revealed delayed endochondral ossification of fore- and hindlimb stylopod elements in mice lacking *Fgf9* (Figs. 4A–D, G–J). Normally, at E15.5, the primary ossification center in the humerus has formed; however, at this stage, the diaphysis of the $Fgf9^{-/-}$ humerus contained predominantly hypertrophic chondrocytes with a narrow zone of vascularization (Figs. 4A, B). In the hindlimb at E15.5, blood vessels were visible in the

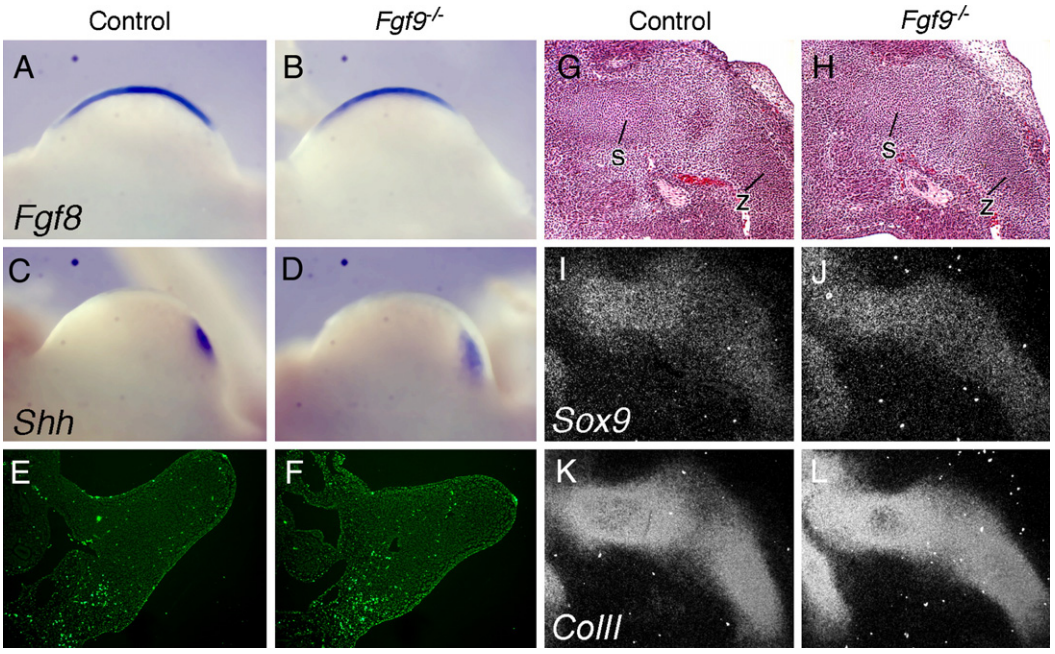

Fig. 3. Loss of *Fgf9* from the AER does not affect limb bud development. (A, B) *Fgf8* expression in the AER of E10.5 control (A) and $Fgf9^{-/-}$ (B) hindlimb buds visualized by whole-mount *in situ* hybridization (WISH). (C, D) *Shh* expression in the AER of E10.5 control (C) and $Fgf9^{-/-}$ (D) hindlimb buds visualized by WISH. (A–D) Dorsal view, anterior to the left, posterior to the right. (E, F) TUNEL staining on transverse sections through E11.5 embryos at the level of the hindlimb bud showing similar levels of apoptosis in control (E) and $Fgf9^{-/-}$ (F) hindlimbs; dorsal at the bottom, proximal to the left. (G, H) Control (G) and $Fgf9^{-/-}$ (H) H&E-stained E12.5 longitudinal hindlimb sections showing similar condensation sizes for proximal and intermediate limb elements. z, zeugopod; s, stylopod. (I, J) *Sox9 in situ* hybridization of nearby sections to panels G and H. (K, L) *ColII in situ* hybridization of nearby sections to panels G and H. (I–L) Dark-field images.

control femoral diaphysis, but the $Fgf9^{-/-}$ femur remained avascular with relatively few hypertrophic chondrocytes (Figs. 4C, D). By E16.5 the primary ossification center had formed in the control femur, while the shaft of the $Fgf9^{-/-}$ bone contained an expanded zone of hypertrophic chondrocytes with a small focus of vascularization and absent trabecular bone formation (Figs. 4G, H). By E18.5 the ossification center in the $Fgf9^{-/-}$ femur was well-developed with abundant blood vessels, although the trabecular bone region was reduced in size (Figs. 4I, J). Delayed bone formation was not apparent in the intermediate and distal elements of the $Fgf9^{-/-}$ limbs (Figs. 4E, F and data not shown).

In vitro studies have shown that FGF9 can activate the c splice forms of FGFRs 1, 2 and 3, FGFR4, and the b splice form of FGFR3 (Ornitz et al., 1996; Zhang et al., 2006). In developing bone, *Fgfrs 1* and *2* are expressed in the mesenchymal condensation, immature and reserve zone chondrocytes, the perichondrium/periosteum and various stages of osteoblast development (Jacob et al., 2006; Ornitz and Marie, 2002; Yu et al., 2003). *Fgfr1* is also expressed in hypertrophic chondrocytes and *Fgfr3* is expressed in proliferating chondrocytes (Ornitz and Marie, 2002) and mature osteoblasts (Xiao et al., 2004). Since *Fgf9* is widely expressed in the perichondrium/periosteum, trabecular bone, surrounding muscle and soft tissue, it can potentially interact with all three *Fgfrs*. To ascertain which FGFR(s) could serve as the physiological receptor for FGF9, we compared the histological phenotype from limbs of $Fgfr3^{-/-}$ mice and from conditional knockout mice lacking *Fgfr1* ($Fgfr1^{cko}$) or *Fgfr2* ($Fgfr2^{cko}$) in osteochondroblast lineages with those of $Fgf9^{-/-}$ mice. These studies revealed that $Fgfr1^{cko}$ mice exhibited a consistent delay in hypertrophic cartilage differentiation at mid-embryonic stages (Fig. 4L), similar to that observed in the $Fgf9^{-/-}$ mice, while $Fgfr2^{cko}$ mice (Fig. 4M) or $Fgfr3^{-/-}$ mice (Fig. 4N) did not exhibit histomorphological alterations at this stage.

Delayed initiation of chondrocyte hypertrophy in $Fgf9^{-/-}$ mice

The narrowed zone of hypertrophic chondrocytes observed in the $Fgf9^{-/-}$ femur at E15.5 (Figs. 4C, D) suggested that chondrocyte maturation might be defective in proximal skeletal elements. To examine chondrogenesis in the mutant limbs, expression studies were performed for *ColII*, a marker of proliferating chondrocytes, and type X collagen (*ColX*), a specific marker of hypertrophic chondrocytes. At E14.5, *ColII* expression was present throughout the control femur, except in the central region of the cartilage, where chondrocytes had undergone hypertrophy. Cells with downregulated *ColII* expression showed high levels of *ColX* mRNA (Figs. 5A, C, E). In the $Fgf9^{-/-}$ femur at the same stage, *ColII* expression was present throughout the entire cartilage anlagen while *ColX* expression was completely absent, indicating that chondrocytes had not yet matured to the hypertrophic stage (Figs. 5B, D, F). A decrease in the pool of proliferating chondrocytes available to undergo hypertrophic differentiation could explain the observed delay in chondrocyte maturation. BrdU incorporation studies to assess cell proliferation rates at E13.5 and E14.5 showed a significant reduction in proliferation of $Fgf9^{-/-}$ femoral chondrocytes at E14.5 compared to control (Table 1). At E13.5, no significant difference in proliferation was detected.

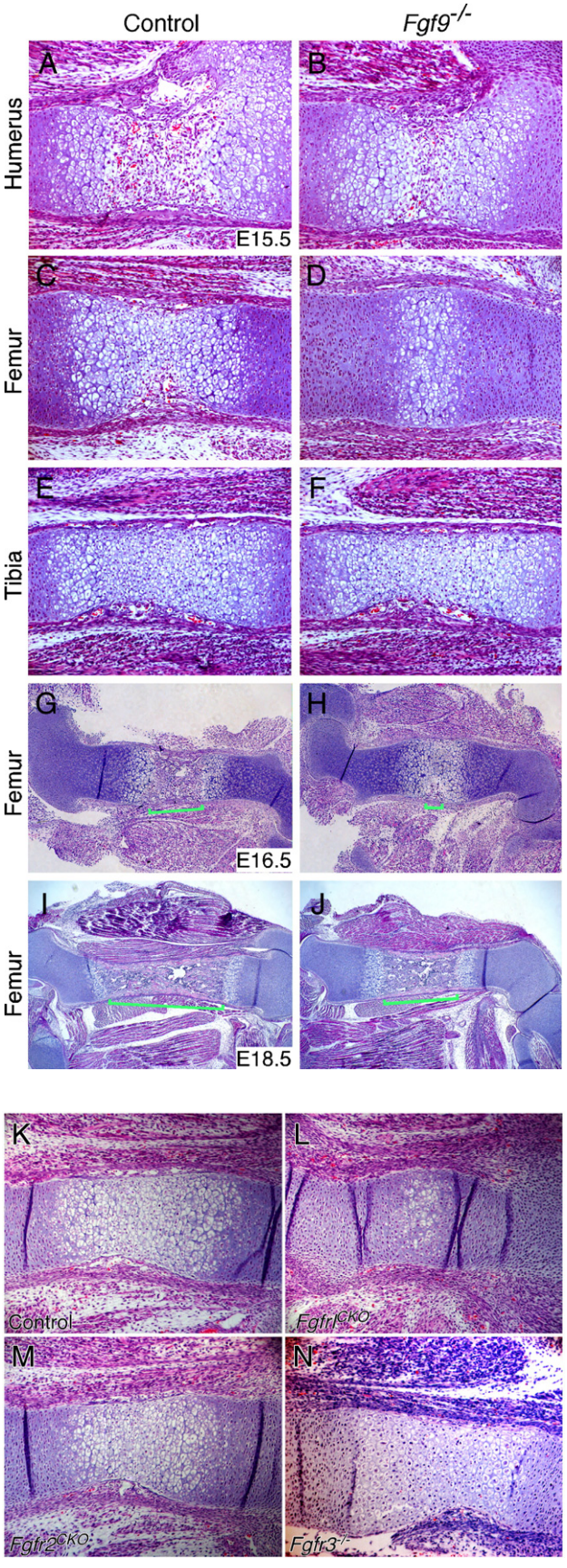

At late stages of embryogenesis (E17.5–18.5), *ColII* and *ColX* expression levels were similar between the control and $Fgf9^{-/-}$ distal femoral growth plates (Figs. 5I–L); however, the hypertrophic zone (HZ) height was significantly enlarged in the $Fgf9^{-/-}$ femora (Figs. 5G, H, Table 2). In contrast, the hypertrophic zone height in the proximal tibia did not differ significantly between $Fgf9^{-/-}$ and control mice (Table 2). The expanded hypertrophic chondrocyte zone in the $Fgf9^{-/-}$ femur could result from increased proliferation, in effect enlarging the pool of precursor chondrocytes available to undergo hypertrophy, a reduction in the rate of loss of terminally differentiated hypertrophic chondrocytes, or a delay in the initiation of chondrocyte loss due to delayed formation of the primary ossification center.

Ihh and PTHrP signaling are delayed during early chondrogenesis in $Fgf9^{-/-}$ mice

Consistent with these findings, the patterns of expression for *Ihh*, *Ptc* and *Pth1r* expression suggested delayed chondrocyte differentiation in the $Fgf9^{-/-}$ femur at E14.5 (Fig. 6). For example, *Ihh* is normally expressed in prehypertrophic chondrocytes of developing bone, which flank the centrally located hypertrophic chondrocytes of the control femur in two distinct zones at E14.5. In the $Fgf9^{-/-}$ cartilage, *Ihh* is expressed in the prehypertrophic chondrocytes, but these cells are only found in the center of the anlagen (Figs. 6C, D). Similarly, *Ptc* is normally expressed in proliferating and prehypertrophic chondrocytes and the perichondrium, while its expression is downregulated in hypertrophic chondrocytes. In the control femur at this stage, *Ptc* expression is evident in the perichondrium as well as in the populations of proliferating and prehypertrophic chondrocytes that flank the centrally located hypertrophic chondrocytes. However, in the $Fgf9^{-/-}$ femur, expression of *Ptc* appears diffusely throughout the cartilage anlagen and in the perichondrium, with no central area of downregulation due to the absence of mature hypertrophic chondrocytes (Figs. 6E, F). Expression of *Pth1r* is barely detectable in the $Fgf9^{-/-}$ femur at this stage (Figs. 6G, H), while it is easily detected in the control prehypertrophic and hypertrophic chondrocyte populations. By E18.5 (Figs. 6K–P), patterns and levels of *Ihh*, *Ptc* and *Pth1r*

Fig. 4. Histological analysis of $Fgf9^{-/-}$ hindlimbs. (A–F) H&E sections of E15.5 humeri (A, B), femora (C, D) and tibiae (E, F). (A, C, E) control, (B, D, F) $Fgf9^{-/-}$. Note reduced area of vascular invasion in $Fgf9^{-/-}$ humerus. In $Fgf9^{-/-}$ femur, the hypertrophic chondrocyte zone is shortened and no vascular invasion of the cartilage is visible. Development of the $Fgf9^{-/-}$ tibia is similar to the control indicating no developmental delay. (G, H) H&E staining of E16.5 control (G) and $Fgf9^{-/-}$ (H) femora. Note that the primary ossification center has developed in the control bone while only the initial stages of vascular invasion are apparent in $Fgf9^{-/-}$ bone. (I, J) H&E sections of E18.5 control (I) and $Fgf9^{-/-}$ (J) femora. Ossification centers are now well-developed in control and $Fgf9^{-/-}$ bones, but the $Fgf9^{-/-}$ femur is shorter and broader with decreased areas of trabecular bone formation and an enlarged hypertrophic chondrocyte zone. Trabecular bone regions are indicated with green brackets in panels G–J. (K–N) H&E sections of E14.5–E14.75 control (K), $Fgfr1^{cko}$ (L), $Fgfr2^{cko}$ (M) and $Fgfr3^{-/-}$ (N) femora showing a smaller hypertrophic chondrocyte zone in tissue missing *Fgfr1* but not *Fgfr2* or *Fgfr3*.

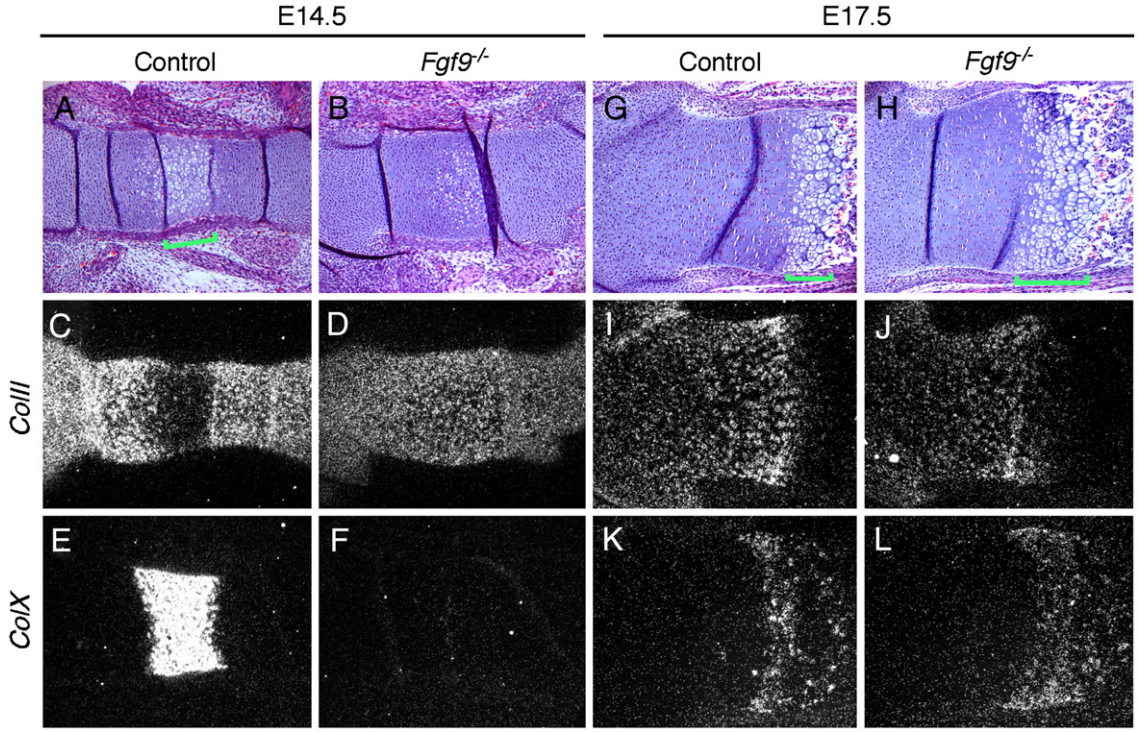

Fig. 5. Expression of chondrocyte differentiation markers at E14.5 and E17.5. H&E staining of E14.5 (A, B) and E17.5 (G, H) femora. *Type II collagen* (*ColII*) expression at E14.5 (C, D) and E17.5 (I, J). *Type X collagen* (*ColX*) expression at E14.5 (E, F) and E17.5 (K, L). Hypertrophic zone regions are indicated with green brackets in panels A, G, H. A, C, E, G, I, K are sections from control littermates. Panels B, D, F, H, J, L are sections from *Fgf9*$^{-/-}$ mice.

expression in *Fgf9*$^{-/-}$ mice were similar to controls, indicating that chondrogenesis at later stages of bone development was not significantly affected by loss of FGF9.

FGF9 promotes osteogenesis in the stylopod

The reduced area of Alizarin red-staining and delayed formation of the primary ossification centers suggested abnormal osteogenesis in *Fgf9*$^{-/-}$ mice. Consistent with our previous findings, von Kossa staining showed abundant mineralization in control bones but significantly decreased mineralization of both trabecular and cortical regions in *Fgf9*$^{-/-}$ bones at E16.5 (Figs. 7A, B and data not shown). Defective osteoblastogenesis is one potential cause for delayed bone formation in *Fgf9*$^{-/-}$ mice and may be due to a deficiency in osteoblast progenitor cells or a defect in osteoblast proliferation or maturation. To characterize osteoblast development, the expression of osteoblast differentiation markers, *Runx2* (*Cbfa1*), *Type I collagen* (*ColI*), and *Osteocalcin* were examined. *Runx2* is expressed in osteoprogenitor cells in the perichondrium and in hypertrophic chondrocytes. Similar levels of expression of *Runx2* were detected in control and *Fgf9*$^{-/-}$ perichondrium at E14.5, indicating that similar numbers of osteoprogenitor cells were present (Figs. 7E, F). However, *ColI* and *Osteocalcin* levels were markedly decreased in the perichondrium/periosteum and trabecular bone regions of *Fgf9*$^{-/-}$ mice from E16.5 to E18.5, which suggested that there were fewer mature osteoblasts in the absence of *Fgf9* (Figs. 7G, H and data not shown). In vitro osteoblast culture data suggest that FGF9 signaling may directly stimulate osteogenic differentiation and matrix mineralization in a stage-dependent manner (Fakhry et al., 2005; Jacob et al., 2006; Valverde-Franco et al., 2004). Thus, FGF9 may function to regulate osteoblast proliferation or differentiation by signaling directly to FGFRs expressed in osteoblast lineages. Alternatively, FGF9 could control the influx of osteoblasts into the trabecular bone region.

Table 1
Cell proliferation in E13.5 and E14.5 control and Fgf9$^{-/-}$ femora

Age	Genotype	*n* [a]	BrdU+cells/0.01 mm^2	*P* value
E13.5	+/+, +/−	7	34.4±1.7	ns
	−/−	4	35.2±1.6	
E14.5	+/+, +/−	6	28.0±2.2	<0.04
	−/−	5	24.5±2.5	

ns, not significant.
[a] *n*, number of animals examined.

Table 2
Bone morphometric data

Growth plate	Genotype	*n* [a]	HZ [b] height (mm)	*P* value
Distal femur	+/+, +/−	3	0.35±0.02	0.001
	−/−	3	0.49±0.01	
Proximal tibia	+/+, +/−	3	0.46±0.03	0.18
	−/−	3	0.50±0.03	

[a] *n*, number of animals examined at E17.5–E18.5.
[b] Hypertrophic chondrocyte zone mean height (mm).

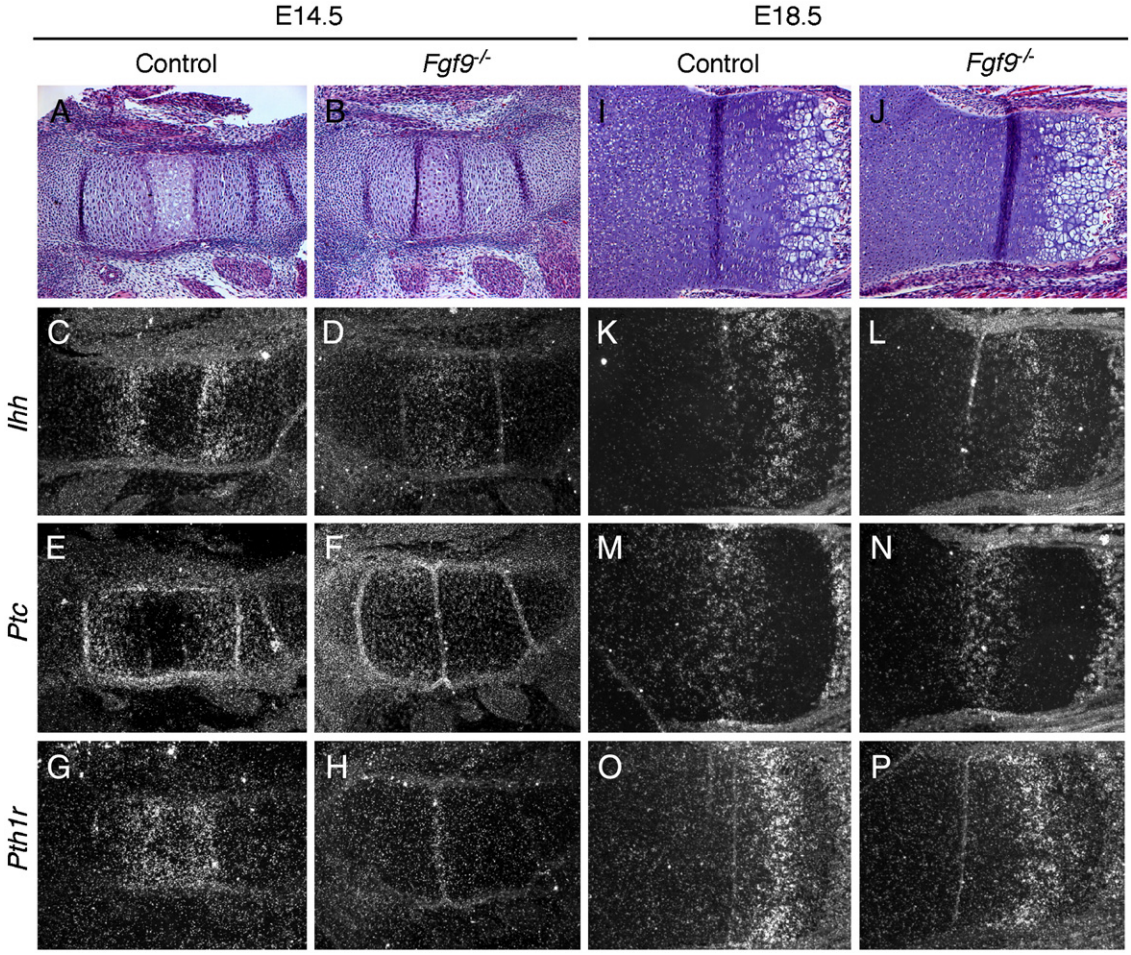

Fig. 6. Expression of *Ihh*, *Ptc* and *Pth1r* at E14.5 and E18.5. H&E staining of E14.5 (A, B) and E18.5 (I, J) femora. (C–H, K–P) Dark-field images. *Ihh* expression at E14.5 (C, D) and E18.5 (K, L). *Ptc* expression at E14.5 (E, F) and E18.5 (M, N). *Pth1r* expression at E14.5 (G, H) and E18.5 (O, P). Panels A, C, E, G, I, K, M, O are sections from control littermates. Panels B, D, F, H, J, L, N, P are sections from *Fgf9*$^{-/-}$ mice.

Deficiency of osteoclasts in Fgf9$^{-/-}$ *bone*

To analyze the osteoclast populations in control and *Fgf9*$^{-/-}$ femurs, *in situ* hybridization studies were performed with the osteoclast-specific markers, matrix metalloproteinase 9 (*MMP9*) and tartrate-resistant acid phosphatase (*TRAP*). At E16.5, *MMP9* expression was localized to the cartilage–bone interface as well as to the trabecular region in control bones, whereas *MMP9* expression was markedly reduced in the *Fgf9*$^{-/-}$ femur, with transcripts detectable only in the vascular invasion front of the developing bone (Figs. 7I, J). *TRAP* expression at E16.5 and TRAP staining at E17.5–E18.5 were similarly decreased in the *Fgf9*$^{-/-}$ femur compared to control (Figs. 7K, L and data not shown). These data indicate that loss of *Fgf9* results in a reduction in osteoclast cell populations in the perichondrium and primary spongiosa of developing bone.

Delayed vascular invasion in Fgf9$^{-/-}$ *femurs*

Vascularization of the developing skeletal elements is a key step in endochondral ossification, allowing the influx of osteoblast and osteoclast progenitors into the initially avascular cartilaginous matrix surrounding hypertrophic chondrocytes (Colnot et al., 2005; Zelzer and Olsen, 2005). Angiogenesis of developing bone was ascertained by PECAM (CD31) immunohistochemistry. At E16.5, blood vessels were present in the perichondrium/periosteum and in the marrow cavity of control femur, while in *Fgf9*$^{-/-}$ mice, blood vessels were clearly visible in the perichondrium surrounding the femur cartilage but had not yet invaded the future marrow cavity (Figs. 8A, B). These data suggest that *Fgf9* is important for promoting skeletal vascularization and that the delayed osteogenesis in the proximal limbs of *Fgf9*$^{-/-}$ mice may result from defects in angiogenesis.

Decreased VEGF signaling in Fgf9$^{-/-}$ *mice*

Vascular endothelial growth factor (VEGF) is essential for blood vessel formation and chondrocyte maturation in the developing skeleton (Maes et al., 2002; Ornitz, 2005; Zelzer et al., 2002; Zelzer and Olsen, 2005). *Vegf* is expressed in the perichondrium and subsequently in hypertrophic chondrocytes and functions to promote vascularization of the cartilage anlagen. In *Fgf9*$^{-/-}$ mice, delayed vascular invasion may be due to decreased VEGF signaling. To test this hypothesis, we exa-

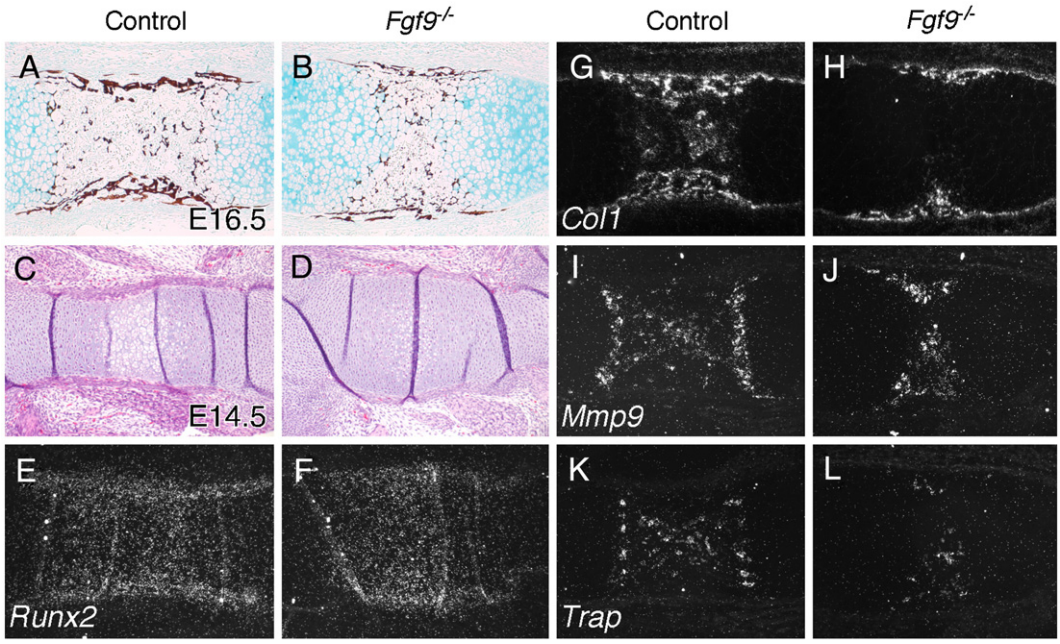

Fig. 7. Osteoblast and osteoclast markers at E14.5 and E16.5. (A, B) von Kossa-stained E16.5 femora. (C, D) H&E-stained E14.5 femora. (E, F) *Runx2/Cbfa1* expression at E14.5. (G, H) *ColI* expression at E16.5. (I, J) *MMP9* expression at E16.5. (K, L) *TRAP* expression at E16.5. (E–L) Dark-field images. Panels A, C, E, G, I, K are sections from control littermates. Panels B, D, F, H, J, L are sections from $Fgf9^{-/-}$ mice.

mined *Vegf* expression in control and $Fgf9^{-/-}$ stylopod elements (Figs. 8C–F). At E14.5, similar levels of *Vegf* expression were observed in the perichondrium. However, in control bone, *Vegf* was also expressed centrally in hypertrophic chondrocytes, whereas in $Fgf9^{-/-}$ mice, there was little *Vegf* expression in this region. *Vegf receptor* (*Vegfr*) expression levels correlate with the intensity of VEGF signaling (Barleon et al., 1997; Gerber et al., 1999; Shen et al., 1998; Zelzer et al., 2002). At E16.5, both *Vegfr1* and *Vegfr2* expression levels were decreased in the perichondrium and diaphysis of $Fgf9^{-/-}$ femora compared to

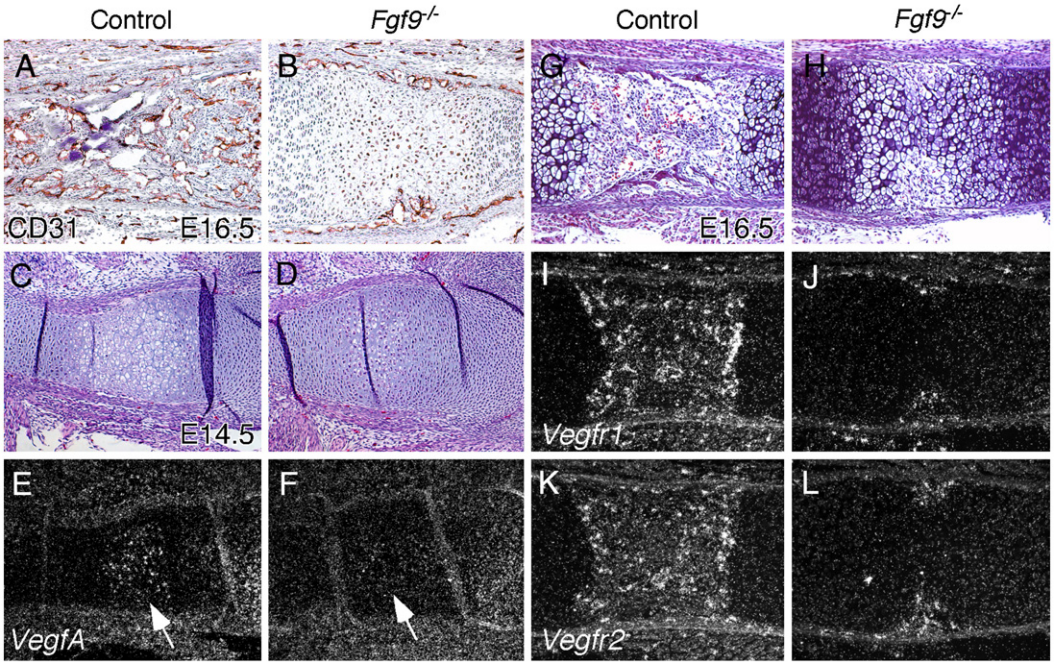

Fig. 8. Vascularization and expression of *Vegf* and *Vegf receptors* in the developing femur. PECAM (CD31) immunohistochemistry (brown signal) counterstained with hematoxylin showing abundant vascularization in control femur (A) compared with $Fgf9^{-/-}$ femur (B) at E16.5. (C, D) H&E staining of E14.5 femora. (E, F) Dark-field images showing *Vegf* expression at E14.5. Note *Vegf* expression in the center of control cartilage anlagen (arrow in E) and in the perichondrium. In $Fgf9^{-/-}$ femur, *Vegf* transcripts are only detectable in the perichondrium (F). (G, H) H&E staining of E16.5 femora. (I–L) Dark-field images showing *Vegfr1* (I, J) and *Vegfr2* (K, L) expression at E16.5. Panels A, C, E, G, I, K are sections from control littermates. Panels B, D, F, H, J, L are sections from $Fgf9^{-/-}$ mice.

control, consistent with decreased *Vegf* expression in the cartilage at E14.5 and reduced vascular invasion of the *Fgf9*$^{-/-}$ hypertrophic zone (Figs. 8I–L).

Fgf9 induces Vegf expression and skeletal vascularization in limb explant cultures

Analyses of *Fgf9*$^{-/-}$ limbs suggest that FGF9 promotes vascular development by stimulating VEGF signaling in proximal skeletal elements. To test whether FGF9 was sufficient to induce *Vegf* expression, E14.5 forelimbs from mice heterozygous for a *ß*-galactosidase-tagged allele of *Vegf* were cultured with bovine serum albumin (BSA), FGF10 or FGF9. *Vegf* expression levels were not affected by treatment with BSA or FGF10, which signals to epithelial FGFR2b; however, *Vegf* expression levels were upregulated in limbs treated with FGF9 (Figs. 9A–C). Cryosections revealed increased *Vegf* expression in the thickened perichondrium and hypertrophic chondrocytes of FGF9-treated explants (Figs. 9D–F). These data demonstrate that FGF9 is sufficient to induce VEGF in skeletal tissue. Since VEGF is an important stimulator of skeletal angiogenesis, these data support the hypothesis that FGF9 regulates vascularization of developing bone by positively regulating *Vegf* expression. PECAM immunohistochemistry was performed on contralateral cartilage explants to determine whether treatment with FGF9 could promote vascularization. Explants cultured with FGF10 did not show an increase in vascularization compared with the BSA control. In contrast, explants cultured with FGF9 showed a marked increase in perichondrial vascularization (Figs. 9G–L).

Discussion

Here we present evidence that FGF9 participates in multiple steps of endochondral ossification to regulate skeletal development in the proximal limb. Mice lacking FGF9 have rhizomelic limb shortening, initiated at the earliest stages of skeletal growth. In *Fgf9*$^{-/-}$ mice, this limb deformity is a consequence of loss of *Fgf9* expression in the muscle, perichondrium/periosteum, trabecular bone and loose mesenchyme surrounding the developing bone rather than loss of *Fgf9* expression in the AER, since development of limb buds and mesenchymal condensations was normal. Analysis of *Fgf9*$^{-/-}$ limbs revealed that, in stylopod elements, loss of FGF9 function resulted in decreased chondrocyte proliferation, delayed initiation of chondrocyte hypertrophy and aberrant formation of mineralized bone secondary to defects in skeletal angiogenesis.

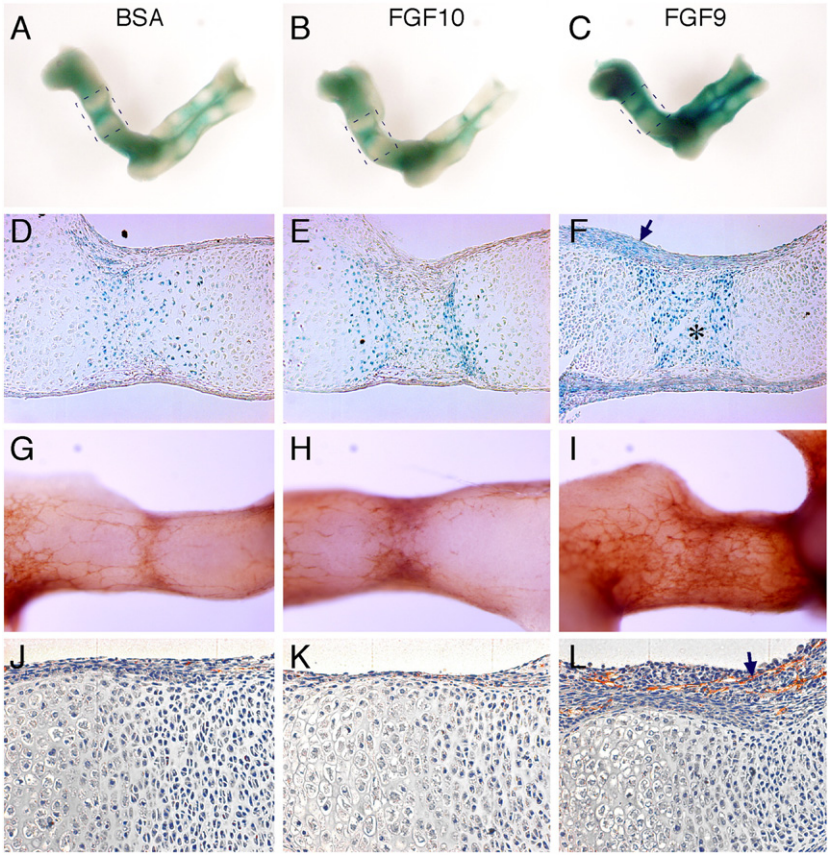

Fig. 9. FGF9 induces *Vegf* expression and vascular development in limb explant cultures. E14.5 forelimb cartilage explants from heterozygous *Vegf-LacZ* embryos were cultured with BSA (A, D, G, J), FGF10 (B, E, H, K) or FGF9 (C, F, I, L). (A–C) staining for *β*-galactosidase enzymatic activity as a measure of *Vegf* expression. (D–F) Frozen sections of boxed areas in panels A–C showing increased β-galactosidase activity in the thickened perichondrium (arrow in panel F) and hypertrophic chondrocytes of the explant cultured with FGF9 (asterisk in panel F). (G–I) PECAM immunohistochemistry (brown signal) on contralateral explants to those shown in panels A–C. Note marked increase in perichondrial vascularization of the explant cultured with FGF9 (I). (J–K) Paraffin sections of panels G–H counterstained with hematoxylin to show FGF9-induced perichondrial vascularization and thickening (arrow in panel L).

FGF9 signaling regulates early stages of chondrogenesis

In the proximal limb elements of *Fgf9*$^{-/-}$ mice, the hypertrophic zone size was decreased at midgestation, suggesting that FGF9 signaling is required for normal chondrocyte maturation. A similar histological phenotype has been observed throughout the skeleton in mice lacking FGF18. In vitro studies have shown that both FGF9 and FGF18 are able to activate all FGFRs expressed in bone (Ornitz et al., 1996; Zhang et al., 2006). To determine which FGFR was transducing the FGF9 signal, growth plate histology was examined from *Fgfr3*$^{-/-}$ mice and from mice lacking FGFR1 or FGFR2 in skeletal lineages. Only the *Fgfr1*^{cko} mice showed a similar decrease in hypertrophic zone size at this stage, indicating that FGF9 likely signals through FGFR1 to initiate hypertrophic chondrocyte differentiation during very early stages of chondrogenesis.

The smaller zone of chondrocyte hypertrophy at early stages in *Fgf9*$^{-/-}$ mice may be due to decreased chondrocyte proliferation at E14.5, which would result in fewer chondrocytes available to undergo differentiation. Reduced proliferation was also observed in *Fgf18*$^{-/-}$ mice (Liu et al., 2007). At earlier stages of chondrogenesis, effects on proliferation in *Fgf9*$^{-/-}$ proximal limbs may be partially masked by redundancy with FGF18 (Davidson et al., 2005; Iwata et al., 2000; Liu et al., 2002, 2007; Ohbayashi et al., 2002). In addition to direct regulation of chondrocyte growth and differentiation by FGF signaling, other pathways known to be important in chondrogenesis, such as the IHH and PTHrP signaling pathways, may also modulate chondrocyte proliferation in response to changes in FGF signaling. During early chondrogenesis, IHH regulates chondrocyte maturation through induction of PTHrP (St-Jacques et al., 1999) and also promotes chondrocyte proliferation through a PTHrP-independent pathway (Karp et al., 2000). In the stylopod elements of *Fgf9*$^{-/-}$ mice at E14.5, *Ihh*, *Ptc* and *Pth1r* expression levels were decreased, suggesting that FGF9 may also regulate chondrogenesis indirectly through these pathways. Reduced levels of *Ihh* were also observed at early stages in *Fgf18*$^{-/-}$ limbs (Liu et al., 2007). Previous studies showed that FGF18 and FGFR3 inhibited *Ihh* expression in prehypertrophic chondrocytes at late embryonic and postnatal stages (Liu et al., 2002, 2007; Naski et al., 1998). Our observations of the concomitant decreases in both *Ihh* expression and chondrocyte proliferation suggest that FGF9 and FGF18 may also regulate chondrocyte proliferation and differentiation indirectly by regulating IHH signaling. In support of this model, Iwata et al. (2000) observed increased chondrocyte proliferation and increased *Ptc* expression at E15.5 in mice harboring an *Fgfr3* gain of function mutation.

FGF9 promotes skeletal vascularization and osteogenesis

In *Fgf9*$^{-/-}$ mice, abnormalities in Alizarin red and von Kossa staining were consistent with decreased mineralization of the femora, suggesting that FGF9 positively regulates osteogenesis in the developing stylopod. Defective bone formation was further confirmed by the observation that osteoblast and osteoclast markers were downregulated in *Fgf9*$^{-/-}$ mice. These findings may be a result of earlier defects in chondrogenesis, or alternatively FGF9 may directly regulate osteogenesis, as has been demonstrated by *in vitro* culture studies (Fakhry et al., 2005). Osteoblasts are derived from mesenchymal progenitor cells that reside in the perichondrium, while osteoclasts originate from hematopoietic lineages. Although it is possible that loss of FGF9 signaling results in independent effects on these two distinct cell lineages, a simpler explanation for the reduced numbers of osteoblasts and osteoclasts in the developing bone is that skeletal angiogenesis, which is required for both of these cell populations to gain entry into the avascular cartilaginous tissue, is delayed in the absence of FGF9. In support of this model, PECAM immunohistochemistry showed delayed vascularization of *Fgf9*$^{-/-}$ stylopod elements. A delay in the formation of the primary spongiosa could also explain the increased hypertrophic zone size observed at late embryonic stages since accumulation of hypertrophic chondrocytes has been reported in several mouse models with impaired skeletal angiogenesis and is thought to result from delayed removal of terminally differentiated hypertrophic chondrocytes (Gerber et al., 1999; Haigh et al., 2000; Vu et al., 1998).

Blood vessel formation is a complex process which is orchestrated by multiple signaling pathways. Various angiogenic factors, including FGF, VEGF, angiopoietins and IHH, are involved in vascularization of the developing skeleton (Colnot et al., 2005; Liu et al., 2007; Zelzer and Olsen, 2005). Several explanations could account for the delayed vascular invasion of the *Fgf9*$^{-/-}$ stylopod growth plates. FGF signaling promotes growth of vascular endothelium (Auguste et al., 2003; Kanda et al., 2004; Seghezzi et al., 1998) and could act directly on endothelial cells to facilitate their invasion of the growth plate. However, conditional inactivation of *Fgfr1* and *Fgfr2* in endothelial cells did not affect skeletal development (KJL and DMO, unpublished observation), suggesting that FGFs do not signal directly to the endothelial cells in the developing growth plate. FGF signaling can also promote *Vegf* expression, either directly or indirectly through other signaling pathways (Kanda et al., 2004; Lavine et al., 2006; Seghezzi et al., 1998). Consistent with this possibility, *Vegf* expression was reduced in the absence of FGF9. Additionally, in forelimb cartilage explant cultures, FGF9 was sufficient to induce *Vegf* expression and to stimulate cell proliferation and vascular growth within the perichondrium (a prerequisite for invasion of the growth plate). Mice lacking *Fgfr3* showed reduced expression of *Vegf* in their expanded zone of hypertrophic chondrocytes and impaired blood vessel formation at the chondro-osseous junction (Amizuka et al., 2004); however, *Fgfr3*$^{-/-}$ mice did not show a delay in the formation of the primary ossification center (Colvin et al., 1996). These data suggest that, during skeletal development, FGF9 signals to FGFR1 and/or FGFR2 in the perichondrium/periosteum to potentiate VEGF signaling and to promote perichondrial angiogenesis. Additionally, FGF9 may signal to FGFR3 in proliferating chondrocytes and/or to FGFR1 in hypertrophic chondrocytes to upregulate VEGF signaling within the growth plate. This source of VEGF would stimulate vascularization of the hypertrophic cartilage and the chondro-osseous junction once the primary ossification center

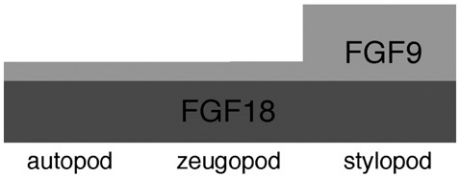

Fig. 10. Functional gradient model of FGF9 and FGF18 in the developing limb. Levels of FGF9 function vary throughout the limb, with highest levels in the stylopod and diminishing levels in more distal segments. In contrast, FGF18 function remains relatively constant throughout the stylopod, zeugopod and autopod compartments.

has been established (Zelzer et al., 2002; Zelzer and Olsen, 2005).

Gradient model for FGF9 and FGF18 in the developing limb

Three FGF ligands, FGFs 2, 9 and 18, have identified physiological roles in skeletogenesis. FGF2 signaling affects trabecular bone architecture but not the onset of ossification or vascularization (Montero et al., 2000). *Fgf9* and *Fgf18* display some overlap in their expression patterns and mice lacking either FGF9 or FGF18 have delayed chondrogenesis, skeletal vascularization and mineralization. However, loss of FGF9 causes a specific defect in the formation of the stylopod elements despite the fact that *Fgf9* is expressed throughout the developing limb, while loss of FGF18 causes a more uniform delay, affecting proximal, intermediate and distal compartments of the developing limb (Liu et al., 2007). These differences may occur because there is an increased dosage requirement of FGFs for development of proximal versus distal limb elements or because different FGF ligands exhibit different levels of activity depending on their location. Based on our data, a model can be proposed in which functional gradients of FGF9 and FGF18 activity modulate various aspects of skeletal development along a proximal-distal axis. This model predicts, for example, that a delayed vascularization phenotype observed in the stylopod in $Fgf9^{-/-}$ embryos may become more severe in the stylopod and extend more distally if one copy of *Fgf18* is removed. Alternatively, the $Fgf18^{-/-}$ phenotype may become more severe if one copy of *Fgf9* is removed. Preliminary observations of these genetic crosses suggest that this type of functional redundancy does occur (Fig. 10).

Another interesting feature of the $Fgf9^{-/-}$ phenotype is the disproportionate shortening of the proximal skeletal elements (rhizomelia). Rhizomelia is a prominent deformity seen in patients with achondroplasia who harbor gain of function mutations in *Fgfr3*. Interestingly, this proximal limb defect has not been observed in mice with activating mutations in *Fgfr3* (Chen et al., 1999, 2001; Iwata et al., 2001; Li et al., 1999; Naski et al., 1998; Segev et al., 2000; Wang et al., 1999) but has been observed postnatally in transgenic mice overexpressing *Fgf9* in cartilage (Garofalo et al., 2003). Furthermore, in $Fgfr3^{-/-}$ mice, the limb overgrowth phenotype is only seen beginning at late embryonic stages, whereas the rhizomelia observed in $Fgf9^{-/-}$ mice occurs at earlier stages. Because signaling through FGFR3 may have a biphasic response during development, it is possible that loss of FGF9 would result in increased proximal limb growth at postnatal stages. If this were the case, specifically inhibiting FGF9 postnatally may provide a therapeutic avenue for the treatment of achondroplasia.

Acknowledgments

We thank G. Schmid, C. Smith and L. Li for technical assistance. VEGF-*LacZ* mice were kindly provided by A. Nagy. Plasmids used for generating digoxigenin-labeled riboprobes were generously provided by G. Martin (*Fgf8*) and A. McMahon (*Shh*). The plasmids used for generating ^{33}P-labeled riboprobes were generously provided by P. Koopman (*Sox9*),Y. Yamada (*type II collagen*), M. Scott (*patched*), A. McMahon (*Ihh*), K. Nakashima (*Runx2/Cbfa1*), E. Vuorio (*type I collagen*), J. Wozney (*Osteocalcin*), G. Andersson (*TRAP*), Z. Werb (*MMP9*), G. Karsenty (*Vegf*) and B. Olsen (*type X collagen*, *Vegfr1,2*). This work was supported by NIH grant HD049808 and NIH NRSA 1-T32-HD043010.

References

Amizuka, N., Davidson, D., Liu, H., Valverde-Franco, G., Chai, S., Maeda, T., Ozawa, H., Hammond, V., Ornitz, D.M., Goltzman, D., Henderson, J.E., 2004. Signalling by fibroblast growth factor receptor 3 and parathyroid hormone-related peptide coordinate cartilage and bone development. Bone 34, 13–25.

Auguste, P., Javerzat, S., Bikfalvi, A., 2003. Regulation of vascular development by fibroblast growth factors. Cell Tissue Res. 314, 157–166.

Barleon, B., Siemeister, G., Martiny-Baron, G., Weindel, K., Herzog, C., Marme, D., 1997. Vascular endothelial growth factor up-regulates its receptor fms-like tyrosine kinase 1 (FLT-1) and a soluble variant of FLT-1 in human vascular endothelial cells. Cancer Res. 57, 5421–5425.

Bateman, N., 1954. Bone growth: a study of the grey-lethal and microphthalmic mutants of the mouse. J. Anat. 88, 212–262.

Bellus, G.A., McIntosh, I., Smith, E.A., Aylesworth, A.S., Kaitila, I., Horton, W.A., Greenhaw, G.A., Hecht, J.T., Francomano, C.A., 1995. A recurrent mutation in the tyrosine kinase domain of fibroblast growth factor receptor 3 causes hypochondroplasia. Nat. Genet. 10, 357–359.

Boulet, A.M., Moon, A.M., Arenkiel, B.R., Capecchi, M.R., 2004. The roles of Fgf4 and Fgf8 in limb bud initiation and outgrowth. Dev. Biol. 273, 361–372.

Britto, J.A., Evans, R.D., Hayward, R.D., Jones, B.M., 2001. From genotype to phenotype: the differential expression of FGF, FGFR, and TGFbeta genes characterizes human cranioskeletal development and reflects clinical presentation in FGFR syndromes. Plast. Reconstr. Surg. 108, 2026–2039 (discussion 2040-6).

Chen, L., Adar, R., Yang, X., Monsonego, E.O., Li, C., Hauschka, P.V., Yayon, A., Deng, C.X., 1999. Gly369Cys mutation in mouse FGFR3 causes achondroplasia by affecting both chondrogenesis and osteogenesis. J. Clin. Invest. 104, 1517–1525.

Chen, L., Li, C., Qiao, W., Xu, X., Deng, C., 2001. A Ser(365)→Cys mutation of fibroblast growth factor receptor 3 in mouse downregulates Ihh/PTHrP signals and causes severe achondroplasia. Hum. Mol. Genet. 10, 457–465.

Cohen, M.M.J., 2000. Fibroblast growth factor receptor mutations. In: Cohen, M.M.J., MacLean, R.E. (Eds.), Craniosynostosis, Diagnosis, Evaluation, and Management. Oxford Univ. Press, New York, pp. 77–94.

Colnot, C., de la Fuente, L., Huang, S., Hu, D., Lu, C., St-Jacques, B., Helms, J.A., 2005. Indian hedgehog synchronizes skeletal angiogenesis and perichondrial maturation with cartilage development. Development 132, 1057–1067.

Colvin, J.S., Bohne, B.A., Harding, G.W., McEwen, D.G., Ornitz, D.M., 1996. Skeletal overgrowth and deafness in mice lacking fibroblast growth factor receptor 3. Nat. Genet. 12, 390–397.

Colvin, J.S., Feldman, B., Nadeau, J.H., Goldfarb, M., Ornitz, D.M., 1999. Genomic organization and embryonic expression of the mouse fibroblast growth factor 9 gene. Dev. Dyn. 216, 72–88.

Colvin, J.S., White, A., Pratt, S.J., Ornitz, D.M., 2001. Lung hypoplasia and neonatal death in Fgf9-null mice identify this gene as an essential regulator of lung mesenchyme. Development 128, 2095–2106.

Davidson, D., Blanc, A., Filion, D., Wang, H., Plut, P., Pfeffer, G., Buschmann, M.D., Henderson, J.E., 2005. Fibroblast growth factor (FGF) 18 signals through FGF receptor 3 to promote chondrogenesis. J. Biol. Chem. 280, 20509–20515.

de Crombrugghe, B., Lefebvre, V., Nakashima, K., 2001. Regulatory mechanisms in the pathways of cartilage and bone formation. Curr. Opin. Cell Biol. 13, 721–727.

Erlebacher, A., Filvaroff, E.H., Gitelman, S.E., Derynck, R., 1995. Toward a molecular understanding of skeletal development. Cell 80, 371–378.

Fakhry, A., Ratisoontorn, C., Vedhachalam, C., Salhab, I., Koyama, E., Leboy, P., Pacifici, M., Kirschner, R.E., Nah, H.D., 2005. Effects of FGF-2/-9 in calvarial bone cell cultures: differentiation stage-dependent mitogenic effect, inverse regulation of BMP-2 and noggin, and enhancement of osteogenic potential. Bone 36, 254–266.

Finch, P.W., Cunha, G.R., Rubin, J.S., Wong, J., Ron, D., 1995. Pattern of keratinocyte growth factor and keratinocyte growth factor receptor expression during mouse fetal development suggests a role in mediating morphogenetic mesenchymal-epithelial interactions. Dev. Dyn. 203, 223–240.

Garofalo, S., Kliger-Spatz, M., Cooke, J.L., Wolstin, O., Lunstrum, G.P., Moshkovitz, S.M., Horton, W.A., Yayon, A., 1999. Skeletal dysplasia and defective chondrocyte differentiation by targeted overexpression of fibroblast growth factor 9 in transgenic mice. J. Bone Miner. Res. 14, 1909–1915.

Garofalo, A., Naumova, E., Manenti, L., Ghilardi, C., Ghisleni, G., Caniatti, M., Colombo, T., Cherrington, J.M., Scanziani, E., Nicoletti, M.I., Giavazzi, R., 2003. The combination of the tyrosine kinase receptor inhibitor SU6668 with paclitaxel affects ascites formation and tumor spread in ovarian carcinoma xenografts growing orthotopically. Clin. Cancer Res. 9, 3476–3485.

Gerber, H.P., Vu, T.H., Ryan, A.M., Kowalski, J., Werb, Z., Ferrara, N., 1999. VEGF couples hypertrophic cartilage remodeling, ossification and angiogenesis during endochondral bone formation. Nat. Med. 5, 623–628.

Haigh, J.J., Gerber, H.P., Ferrara, N., Wagner, E.F., 2000. Conditional inactivation of VEGF-A in areas of collagen2a1 expression results in embryonic lethality in the heterozygous state. Development 127, 1445–1453.

Hurley, M.M., Abreu, C., Gronowicz, G., Kawaguchi, H., Lorenzo, J., 1994. Expression and regulation of basic fibroblast growth factor mRNA levels in mouse osteoblastic MC3T3-E1 cells. J. Biol. Chem. 269, 9392–9396.

Hurley, M.M., Tetradis, S., Huang, Y.F., Hock, J., Kream, B.E., Raisz, L.G., Sabbieti, M.G., 1999. Parathyroid hormone regulates the expression of fibroblast growth factor-2 mRNA and fibroblast growth factor receptor mRNA in osteoblastic cells. J. Bone Miner. Res. 14, 776–783.

Iwata, T., Chen, L., Li, C., Ovchinnikov, D.A., Behringer, R.R., Francomano, C. A., Deng, C.X., 2000. A neonatal lethal mutation in FGFR3 uncouples proliferation and differentiation of growth plate chondrocytes in embryos. Hum. Mol. Genet. 9, 1603–1613.

Iwata, T., Li, C.L., Deng, C.X., Francomano, C.A., 2001. Highly activated Fgfr3 with the K644M mutation causes prolonged survival in severe dwarf mice. Hum. Mol. Genet. 10, 1255–1264.

Jacob, A.L., Smith, C., Partanen, J., Ornitz, D.M., 2006. Fibroblast growth factor receptor 1 signaling in the osteo-chondrogenic cell lineage regulates sequential steps of osteoblast maturation. Dev. Biol. 296, 315–328.

Kanda, S., Miyata, Y., Kanetake, H., 2004. Fibroblast growth factor-2-mediated capillary morphogenesis of endothelial cells requires signals via Flt-1/vascular endothelial growth factor receptor-1: possible involvement of c-Akt. J. Biol. Chem. 279, 4007–4016.

Karp, S.J., Schipani, E., St-Jacques, B., Hunzelman, J., Kronenberg, H., McMahon, A.P., 2000. Indian hedgehog coordinates endochondral bone growth and morphogenesis via parathyroid hormone related-protein-dependent and -independent pathways. Development 127, 543–548.

Karsenty, G., Wagner, E.F., 2002. Reaching a genetic and molecular understanding of skeletal development. Dev. Cell 2, 389–406.

Laufer, E., Nelson, C.E., Johnson, R.L., Morgan, B.A., Tabin, C., 1994. Sonic hedgehog and Fgf-4 act through a signaling cascade and feedback loop to integrate growth and patterning of the developing limb bud. Cell 79, 993–1003.

Lavine, K.J., White, A.C., Park, C., Smith, C.S., Choi, K., Long, F., Hui, C.C., Ornitz, D.M., 2006. Fibroblast growth factor signals regulate a wave of Hedgehog activation that is essential for coronary vascular development. Genes Dev. 20, 1651–1666.

Lewandoski, M., Sun, X., Martin, G.R., 2000. Fgf8 signalling from the AER is essential for normal limb development. Nat. Genet. 26, 460–463.

Li, C., Chen, L., Iwata, T., Kitagawa, M., Fu, X.Y., Deng, C.X., 1999. A Lys644Glu substitution in fibroblast growth factor receptor 3 (FGFR3) causes dwarfism in mice by activation of STATs and ink4 cell cycle inhibitors. Hum. Mol. Genet. 8, 35–44.

Liu, Z., Xu, J., Colvin, J.S., Ornitz, D.M., 2002. Coordination of chondrogenesis and osteogenesis by fibroblast growth factor 18. Genes Dev. 16, 859–869.

Liu, Z., Lavine, K.J., Hung, I.H., Ornitz, D.M., 2007. FGF18 is required for early chondrocyte proliferation, hypertrophy and vascular invasion of the growth plate. Dev. Biol. 302, 80–91.

Maes, C., Carmeliet, P., Moermans, K., Stockmans, I., Smets, N., Collen, D., Bouillon, R., Carmeliet, G., 2002. Impaired angiogenesis and endochondral bone formation in mice lacking the vascular endothelial growth factor isoforms VEGF164 and VEGF188. Mech .Dev. 111, 61–73.

Mariani, F.V., Martin, G.R., 2003. Deciphering skeletal patterning: clues from the limb. Nature 423, 319–325.

Martin, G.R., 1998. The roles of FGFs in the early development of vertebrate limbs. Genes Dev. 12, 1571–1586.

Maruoka, Y., Ohbayashi, N., Hoshikawa, M., Itoh, N., Hogan, B.M., Furuta, Y., 1998. Comparison of the expression of three highly related genes, Fgf8, Fgf17 and Fgf18, in the mouse embryo. Mech. Dev. 74, 175–177.

Mason, I.J., Fuller-Pace, F., Smith, R., Dickson, C., 1994. FGF-7 (keratinocyte growth factor) expression during mouse development suggests roles in myogenesis, forebrain regionalisation and epithelial–mesenchymal interactions. Mech. Dev. 45, 15–30.

Min, H., Danilenko, D.M., Scully, S.A., Bolon, B., Ring, B.D., Tarpley, J.E., DeRose, M., Simonet, W.S., 1998. Fgf-10 is required for both limb and lung development and exhibits striking functional similarity to Drosophila branchless. Genes Dev. 12, 3156–3161.

Miquerol, L., Gertsenstein, M., Harpal, K., Rossant, J., Nagy, A., 1999. Multiple developmental roles of VEGF suggested by a LacZ-tagged allele. Dev. Biol. 212, 307–322.

Montero, A., Okada, Y., Tomita, M., Ito, M., Tsurukami, H., Nakamura, T., Doetschman, T., Coffin, J.D., Hurley, M.M., 2000. Disruption of the fibroblast growth factor-2 gene results in decreased bone mass and bone formation. J. Clin. Invest. 105, 1085–1093.

Moon, A.M., Capecchi, M.R., 2000. Fgf8 is required for outgrowth and patterning of the limbs. Nat. Genet. 26, 455–459.

Morriss-Kay, G.M., Wilkie, A.O., 2005. Growth of the normal skull vault and its alteration in craniosynostosis: insights from human genetics and experimental studies. J. Anat. 207, 637–653.

Naski, M.C., Ornitz, D.M., 1998. FGF signaling in skeletal development. Front. Biosci. 3, D781–D794.

Naski, M.C., Colvin, J.S., Coffin, J.D., Ornitz, D.M., 1998. Repression of hedgehog signaling and BMP4 expression in growth plate cartilage by fibroblast growth factor receptor 3. Development 125, 4977–4988.

Niswander, L., 2003. Pattern formation: old models out on a limb. Nat. Rev., Genet. 4, 133–143.

Niswander, L., Jeffrey, S., Martin, G.R., Tickle, C., 1994. A positive feedback loop coordinates growth and patterning in the vertebrate limb (see comments). Nature 371, 609–612.

Ohbayashi, N., Shibayama, M., Kurotaki, Y., Imanishi, M., Fujimori, T., Itoh, N., Takada, S., 2002. FGF18 is required for normal cell proliferation and differentiation during osteogenesis and chondrogenesis. Genes Dev. 16, 870–879.

Ohuchi, H., Nakagawa, T., Yamamoto, A., Araga, A., Ohata, T., Ishimaru, Y., Yoshioka, H., Kuwana, T., Nohno, T., Yamasaki, M., Itoh, N., Noji, S., 1997. The mesenchymal factor, FGF10, initiates and maintains the outgrowth of the chick limb bud through interaction with FGF8, an apical ectodermal factor. Development 124, 2235–2244.

Ornitz, D.M., 2005. FGF signaling in the developing endochondral skeleton. Cytokine Growth Factor Rev. 16, 205–213.

Ornitz, D.M., Marie, P.J., 2002. FGF signaling pathways in endochondral and intramembranous bone development and human genetic disease. Genes Dev. 16, 1446–1465.

Ornitz, D.M., Xu, J., Colvin, J.S., McEwen, D.G., MacArthur, C.A., Coulier, F., Gao, G., Goldfarb, M., 1996. Receptor specificity of the fibroblast growth factor family. J. Biol. Chem. 271, 15292–15297.

Orr-Urtreger, A., Givol, D., Yayon, A., Yarden, Y., Lonai, P., 1991. Developmental expression of two murine fibroblast growth factor receptors, flg and bek. Development 113, 1419–1434.

Peters, K., Ornitz, D., Werner, S., Williams, L., 1993. Unique expression pattern of the FGF receptor 3 gene during mouse organogenesis. Dev. Biol. 155, 423–430.

Peters, K.G., Werner, S., Chen, G., Williams, L.T., 1992. Two FGF receptor genes are differentially expressed in epithelial and mesenchymal tissues during limb formation and organogenesis in the mouse. Development 114, 233–243.

Pirvola, U., Ylikoski, J., Trokovic, R., Hebert, J.M., McConnell, S.K., Partanen, J., 2002. FGFR1 is required for the development of the auditory sensory epithelium. Neuron 35, 671–680.

Rousseau, F., Bonaventure, J., Legeal-Mallet, L., Pelet, A., Rozet, J.M., Maroteaux, P., Le Merrer, M., Munnich, A., 1994. Mutations in the gene encoding fibroblast growth factor receptor-3 in achondroplasia. Nature 371, 252–254.

Sabbieti, M.G., Marchetti, L., Abreu, C., Montero, A., Hand, A.R., Raisz, L.G., Hurley, M.M., 1999. Prostaglandins regulate the expression of fibroblast growth factor-2 in bone. Endocrinology 140, 434–444.

Sabbieti, M.G., Marchetti, L., Gabrielli, M.G., Menghi, M., Materazzi, S., Menghi, G., Raisz, L.G., Hurley, M.M., 2005. Prostaglandins differently regulate FGF-2 and FGF receptor expression and induce nuclear translocation in osteoblasts via MAPK kinase. Cell Tissue Res. 319, 267–278.

Segev, O., Chumakov, I., Nevo, Z., Givol, D., Madar-Shapiro, L., Sheinin, Y., Weinreb, M., Yayon, A., 2000. Restrained chondrocyte proliferation and maturation with abnormal growth plate vascularization and ossification in human FGFR-3(G380R) transgenic mice. Hum. Mol. Genet. 9, 249–258.

Seghezzi, G., Patel, S., Ren, C.J., Gualandris, A., Pintucci, G., Robbins, E.S., Shapiro, R.L., Galloway, A.C., Rifkin, D.B., Mignatti, P., 1998. Fibroblast growth factor-2 (FGF-2) induces vascular endothelial growth factor (VEGF) expression in the endothelial cells of forming capillaries: an autocrine mechanism contributing to angiogenesis. J. Cell Biol. 141, 1659–1673.

Shen, B.Q., Lee, D.Y., Gerber, H.P., Keyt, B.A., Ferrara, N., Zioncheck, T.F., 1998. Homologous up-regulation of KDR/Flk-1 receptor expression by vascular endothelial growth factor in vitro. J. Biol. Chem. 273, 29979–29985.

Shiang, R., Thompson, L.M., Zhu, Y.-Z., Church, D.M., Fielder, T.J., Bocian, M., Winokur, S.T., Wasmuth, J.J., 1994. Mutations in the transmembrane domain of FGFR3 cause the most common genetic form of dwarfism, achondroplasia. Cell 78, 335–342.

St-Jacques, B., Hammerschmidt, M., McMahon, A.P., 1999. Indian hedgehog signaling regulates proliferation and differentiation of chondrocytes and is essential for bone formation. Genes Dev. 13, 2072–2086.

Sullivan, R., Klagsbrun, M., 1985. Purification of cartilage-derived growth factor by heparin affinity chromatography. J. Biol. Chem. 260, 2399–2403.

Sun, X., Mariani, F.V., Martin, G.R., 2002. Functions of FGF signalling from the apical ectodermal ridge in limb development. Nature 418, 501–508.

Tavormina, P.L., Shiang, R., Thompson, L.M., Zhu, Y., Wilkin, D.J., Lachman, R.S., Wilcox, W.R., Rimoin, D.L., Cohn, D.H., Wasmuth, J.J., 1995. Thanatophoric dysplasia (types I and II) caused by distinct mutations in fibroblast growth factor receptor 3. Nat. Genet. 9, 321–328.

Valverde-Franco, G., Liu, H., Davidson, D., Chai, S., Valderrama-Carvajal, H., Goltzman, D., Ornitz, D.M., Henderson, J.E., 2004. Defective bone mineralization and osteopenia in young adult FGFR3$^{-/-}$ mice. Hum. Mol. Genet. 13, 271–284.

Vu, T.H., Shipley, J.M., Bergers, G., Berger, J.E., Helms, J.A., Hanahan, D., Shapiro, S.D., Senior, R.M., Werb, Z., 1998. MMP-9/gelatinase B is a key regulator of growth plate angiogenesis and apoptosis of hypertrophic chondrocytes. Cell 93, 411–422.

Wang, Y.C., Spatz, M.K., Kannan, K., Hayk, H., Avivi, A., Gorivodsky, M., Pines, M., Yayon, A., Lonai, P., Givol, D., 1999. A mouse model for achondroplasia produced by targeting fibroblast growth factor receptor 3. Proc. Natl. Acad. Sci. U. S. A. 96, 4455–4460.

Wilkie, A.O.M., 1997. Craniosynostosis—Genes and mechanisms. Hum. Mol. Genet. 6, 1647–1656.

Wilkie, A.O., 2000. Epidemiology and genetics of craniosynostosis. Am. J. Med. Genet. 90, 82–83.

Xiao, L., Naganawa, T., Obugunde, E., Gronowicz, G., Ornitz, D.M., Coffin, J.D., Hurley, M.M., 2004. Stat1 controls postnatal bone formation by regulating fibroblast growth factor signaling in osteoblasts. J. Biol. Chem. 279, 27743–27752.

Xu, J., Lawshe, A., MacArthur, C.A., Ornitz, D.M., 1999. Genomic structure, mapping, activity and expression of fibroblast growth factor 17. Mech. Dev. 83, 165–178.

Yu, K., Xu, J., Liu, Z., Sosic, D., Shao, J., Olson, E.N., Towler, D.A., Ornitz, D.M., 2003. Conditional inactivation of FGF receptor 2 reveals an essential role for FGF signaling in the regulation of osteoblast function and bone growth. Development 130, 3063–3074.

Zelzer, E., Olsen, B.R., 2005. Multiple roles of vascular endothelial growth factor (VEGF) in skeletal development, growth, and repair. Curr. Top. Dev. Biol. 65, 169–187.

Zelzer, E., McLean, W., Ng, Y.S., Fukai, N., Reginato, A.M., Lovejoy, S., D'Amore, P.A., Olsen, B.R., 2002. Skeletal defects in VEGF(120/120) mice reveal multiple roles for VEGF in skeletogenesis. Development 129, 1893–1904.

Zhang, X., Ibrahimi, O.A., Olsen, S.K., Umemori, H., Mohammadi, M., Ornitz, D.M., 2006. Receptor specificity of the fibroblast growth factor family: part II. J. Biol. Chem. 281 (23), 15694–15700 (Jun 9).

Zuniga, A., Haramis, A.P., McMahon, A.P., Zeller, R., 1999. Signal relay by BMP antagonism controls the SHH/FGF4 feedback loop in vertebrate limb buds. Nature 401, 598–602.